

## BIFURCATIONS OF TRANSONIC FLOW PAST SIMPLE AIRFOILS WITH ELLIPTIC AND WEDGE-SHAPED NOSES

A. G. Kuz'min

UDC 533.6.011

*A turbulent transonic flow past two symmetric airfoils with flat midparts is studied numerically. Using the Reynolds-averaged Navier–Stokes equations, we analyze the flow past a 9% thick airfoil with an elliptic nose. A range of the free-stream Mach number  $M_\infty$ , in which flow bifurcations occur, is determined. Values of  $M_\infty$  that give rise to significant changes in the lift coefficient with variations of the angle of attack are specified. Flow bifurcations are also revealed for a thin double wedge, i.e., a sort of a hexagon.*

**Key words:** airfoil, local supersonic regions, buffet, bifurcations.

**Introduction.** The existence of bifurcations of a transonic flow past symmetric and asymmetric airfoils having lengthy portions with a small or zero curvature was established in a number of studies on the basis of the Navier–Stokes equations [1–3]. In [4, 5], we obtained and analyzed regimes of transonic buffet and bifurcations of the flow past simple airfoils whose nose and tail are circular arcs. In this work, the above-mentioned phenomena are studied for other simple airfoils.

**1. Formulation of the Problem and Numerical Method.** We consider a two-dimensional flow past a smooth symmetric airfoil of thickness  $h$  whose midpart is a couple of segments parallel to the  $x$  axis:

$$y(x) = \pm h/2, \quad a \leq x \leq 1 - a. \quad (1)$$

The nose is an elliptic arc:

$$y(x) = \pm(h/2)\sqrt{(2-x/a)x/a} \quad (0 \leq x \leq a), \quad (2)$$

where  $a$  is the length of the nose portion of the airfoil. The tail of the same length as the nose is constituted by two circular arcs of radius  $R = b + h/2$ , where  $b$  is the distance from the circumcenter to the  $x$  axis (Fig. 1):

$$y(x) = \mp b \pm \sqrt{b^2 + a^2 - (x - 1 + a)^2}, \quad 1 - a \leq x \leq 1. \quad (3)$$

As the arcs have a common endpoint  $x = 1$ ,  $y = 0$ , we obtain  $R = (a^2 + b^2)^{1/2}$ . Using the latter expression and the formula  $R = b + h/2$ , we find the relation between the parameters that determine the airfoil tail:  $b = (a^2 - h^2/4)/h$ .

The outer boundary of the lens-type computational domain is composed by two curves  $\Gamma_1$  and  $\Gamma_2$  located at a minimum distance of 40 chord lengths from the airfoil and a maximum distance of 100 chord lengths. On the inflow part  $\Gamma_1$  of the outer boundary, fixed values of the angle of attack  $\alpha$ , Mach number  $M_\infty < 1$ , and static temperature  $T_\infty$  are given. On the outflow part  $\Gamma_2$  of the boundary, we prescribe the static pressure  $p_\infty$  related to the temperature  $T$  and density  $\rho$  by the equation of state  $p = \rho T c_v (\gamma - 1)$ , where  $\gamma = 1.4$ . The no-slip condition and the vanishing heat flux are prescribed on the airfoil (1)–(3). The initial data are either uniform free-stream parameters or a nonuniform flow field obtained previously for other values of  $M_\infty$  and  $\alpha$ .

Solutions of the initial-value problem for the system of Navier–Stokes equations endowed with the SST- $k$ - $\omega$  turbulence model were obtained with a finite-volume solver [4]. A hybrid computational mesh was constituted by quadrangles near the airfoil and by triangles in the rest of the domain. To provide good accuracy of flow simulation

---

St. Petersburg State University, St. Petersburg 198504; alexander.kuzmin@pobox.spbu.ru. Translated from Prikladnaya Mekhanika i Tekhnicheskaya Fizika, Vol. 51, No. 1, pp. 22–28, January–February, 2010. Original article submitted March 11, 2009.

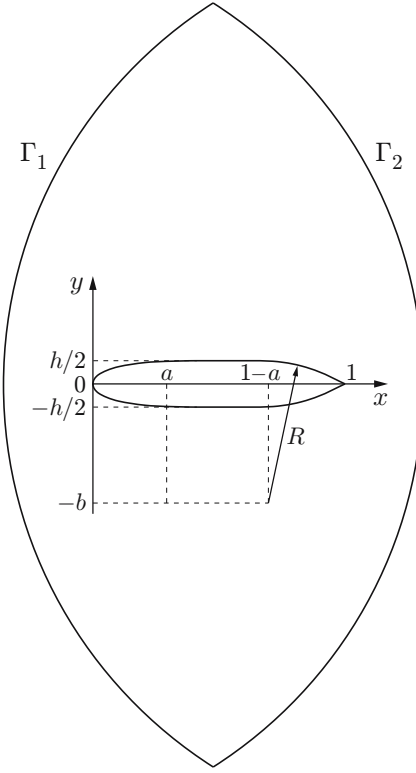


Fig. 1. Sketch of the airfoil and the outer boundary of the computational domain.

in the boundary layer, we chose such positions for the nearest nodes to the airfoil that the dimensionless distance  $y^+$  was less than unity [6]. The total number of mesh nodes was approximately  $1.8 \cdot 10^5$ . The solver was validated by running a few benchmark problems on transonic buffet [4].

**2. Flow Past a 9%-Thick Airfoil with an Elliptic Nose.** For the airfoil (1)–(3) with  $h = 0.09$  and  $a = 0.3$ , we consider the same free-stream conditions as in the case of a 9%-thick airfoil with a sharp nose treated in [5]:  $T_\infty = 250$  K and  $p_\infty = 108,000$  Pa.

Numerical solutions obtained with the above-mentioned solver revealed the existence of flow bifurcations at  $\alpha = 0^\circ$  in the range of the free-stream Mach numbers

$$0.8554 \leq M_\infty \leq 0.8640. \quad (4)$$

Apart from the bifurcations, the solutions showed self-sustained oscillations (buffet onset) due to separation of the boundary layers from the upper and lower surfaces of the airfoil in the aft region. Figure 2 demonstrates the maximum values  $C_{L,\max}$  and minimum values  $C_{L,\min}$  of the lift coefficient for periodic self-sustained oscillations at various values of  $M_\infty$ .

The realization of symmetric or asymmetric flow regimes depends on the initial data and time history of the parameters  $M_\infty$  and  $\alpha$  [4, 5]. The domains I and IV in Fig. 2 correspond to the flow fields obtained for the initial data determined by the uniform free stream and the zero angle of attack; the fields averaged in time are symmetric about the  $x$  axis.

To obtain asymmetric flow fields corresponding to the domain II, we first ran flow computations for the initial data  $M_\infty = 0.86$  and  $\alpha = 1^\circ$ , and then the angle of attack was reduced to  $\alpha = 0^\circ$ . The thus-obtained parameters of the asymmetric flow at  $\alpha = 0^\circ$  were used as the initial data for transonic flow computations at smaller and greater values of  $M_\infty$ . This made it possible to determine the bifurcation interval (4), in which there exist asymmetric flow fields at  $\alpha = 0^\circ$ . Figure 3 shows the asymmetric flow field (with three local supersonic regions) obtained at an instant  $t$  for  $M_\infty = 0.857$  and  $\alpha = 0^\circ$ . In the proximity of the trailing edge, the flow pattern with the boundary

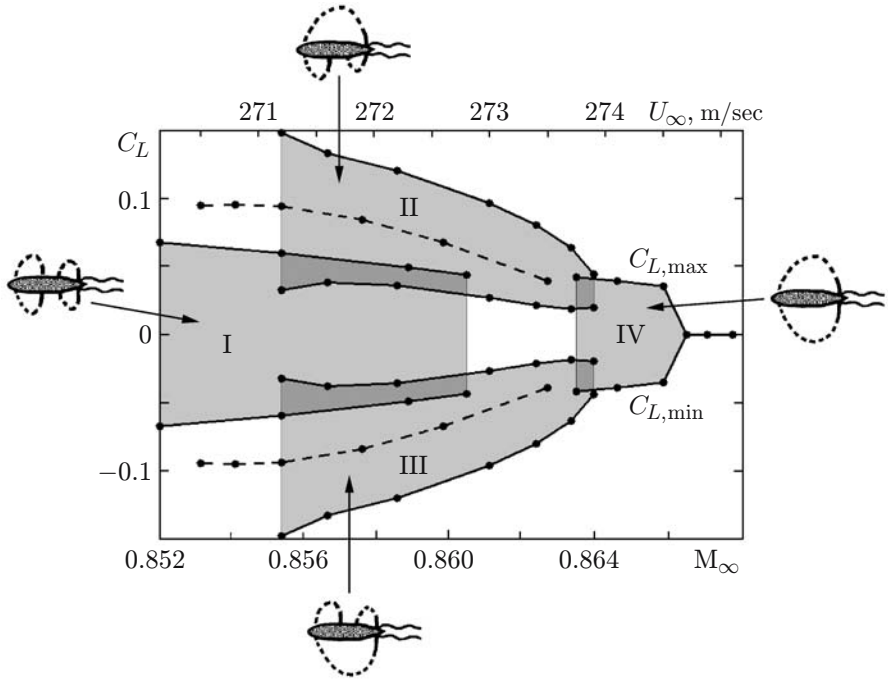


Fig. 2. Maximum and minimum values of the lift coefficient  $C_L$  versus the Mach number  $M_\infty$  for self-sustained flow oscillations about the airfoil (thickness  $h = 0.09$ ) described by Eqs. (1)–(3) at  $a = 0.3$ ,  $\alpha = 0^\circ$ , and  $Re = 1.1 \cdot 10^7$ : the domains indicated by I–IV correspond to flow regimes with different numbers of local supersonic regions: four regions (I), three regions (II and III), and two regions (IV); the dashed curves show the results obtained for the inviscid flow.

layer separation differs only slightly from that studied in [4]. The Reynolds number based on the airfoil chord length of 0.5 m and  $M_\infty \approx 0.86$  is  $1.1 \cdot 10^7$ . The frequency of self-sustained oscillations is 143–147 Hz for the regimes I–III (see Fig. 2) and 137 Hz for the regime IV.

In the interval  $0.8604 < M_\infty < 0.8636$  between the domains I and IV indicated in Fig. 2, the symmetric flow past the airfoil (1)–(3) is unstable. In this interval, perturbations that emanate from the oscillating boundary layers trigger restructuring of the flow field and a transition to an asymmetric flow with three local supersonic regions (and positive or negative lift coefficient). The causes of the instability of the flow structure with local supersonic regions residing closely to each other were discussed in [3–5].

The free-stream Mach number  $M_\infty = 0.8555$  turned out to be the most unfavorable one, as it provokes considerable jumps of the lift coefficient under small perturbations of the angle  $\alpha$ . This follows from the analysis of Fig. 2 and is also confirmed by the dependence of  $C_L$  on  $\alpha$  plotted in Fig. 4. At  $M_\infty = 0.8555$ , it is seen that small reversal oscillations of the angle of attack around  $\alpha = 0^\circ$  may result in jumps of the lift coefficient from  $C_L = -0.15$  to  $C_L = 0.15$ , in contrast to a smooth behavior of  $C_L(\alpha)$  at  $M_\infty = 0.867$ .

The numerical simulations of the flow past the airfoil (1)–(3) with  $a = 0.3$  demonstrated that the bifurcation range in this case virtually coincides with that obtained in [5] for an airfoil whose nose and tail are circular arcs of a smaller length ( $a = 0.25$ ). This is explained by the fact that the lengths of the airfoil midparts with a zero or small local curvature are nearly the same for the two cases mentioned above. On the other hand, replacement of the circular-arc nose by the elliptic-arc nose with the same parameter  $a = 0.25$  would result in a considerable expansion of the airfoil portion with a small curvature and in a displacement of the bifurcation interval toward greater values of  $M_\infty$ .

Computations of the inviscid flow past the airfoil (1)–(3) on the basis of the Euler equations yielded a slight shift of the bifurcation interval toward smaller values of the Mach number (dashed curves in Fig. 2).

**3. Flow Past a Thin Double Wedge of 7% Thickness.** A symmetric double wedge with a rectangular insert is determined by the following expressions:

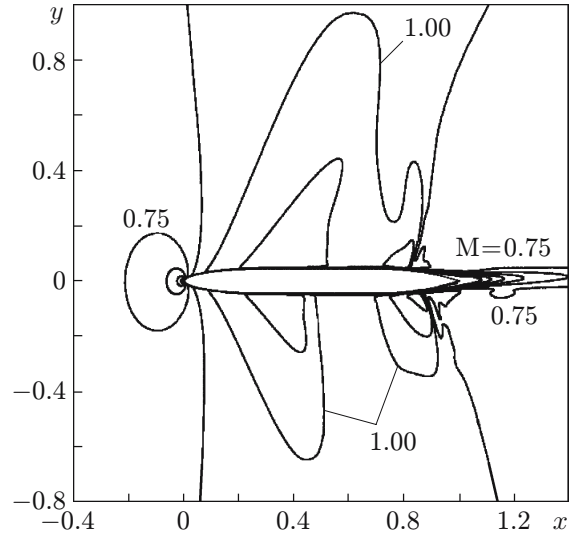


Fig. 3. Mach number contours in an asymmetric flow past the airfoil described by Eqs. (1)–(3) for  $h = 0.09$ ,  $a = 0.3$ ,  $\alpha = 0^\circ$ ,  $M_\infty = 0.857$ , and  $Re = 1.1 \cdot 10^7$ .

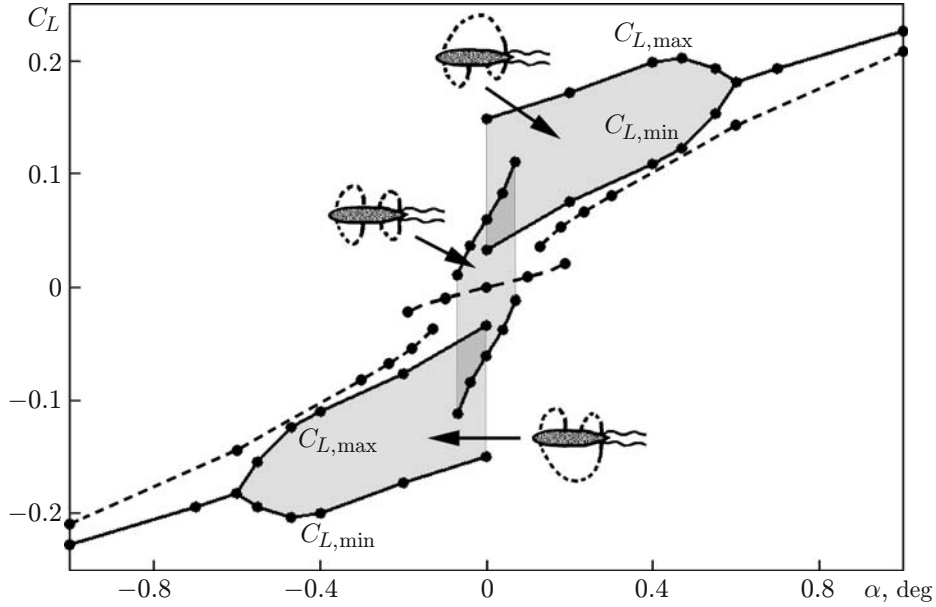


Fig. 4. Maximum and minimum values of the lift coefficient  $C_L$  versus the angle of attack for the airfoil described by Eqs. (1)–(3) for  $h = 0.09$ ,  $a = 0.3$ , and  $Re = 1.1 \cdot 10^7$ : the shaded domains refer to  $M_\infty = 0.8555$ ; the dashed curves refer to  $M_\infty = 0.867$ .

$$y(x) = \begin{cases} \pm h/2, & a \leq x \leq 1-a, \\ \pm hx/(2a), & 0 < x < a, \\ \pm h(1-x)/(2a), & 1-a < x < 1. \end{cases} \quad (5)$$

We choose the same airfoil thickness ( $h = 0.07$ ) and the nose and tail lengths ( $a = 0.3$ ) as those for a smooth airfoil considered in Sec. 3 of the paper [4]. In addition, we prescribe the same free-stream parameters:  $T_\infty = 250$  K and  $p_\infty = 5 \cdot 10^4$  Pa.

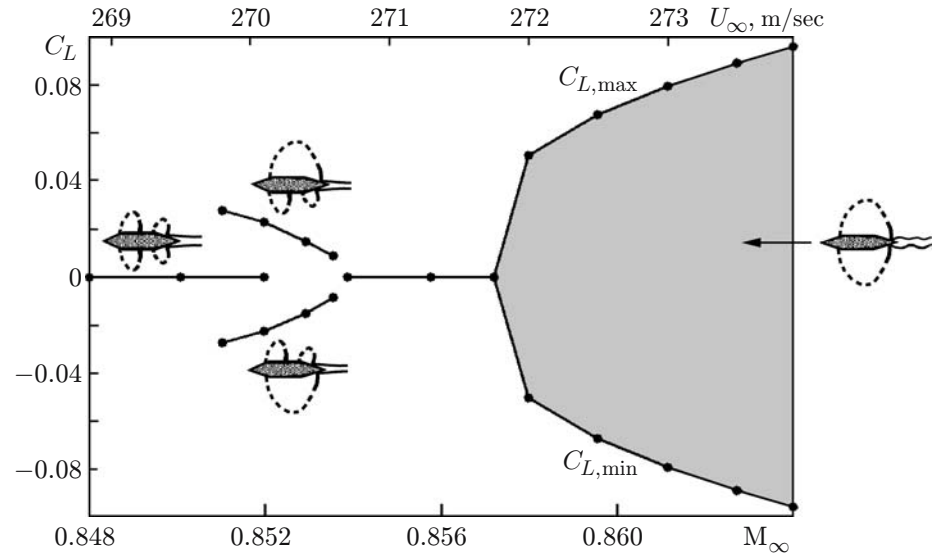


Fig. 5. Maximum and minimum values of the lift coefficient  $C_L$  versus the Mach number  $M_\infty$  for the airfoil described by Eqs. (5) with  $h = 0.07$ ,  $a = 0.3$ ,  $\alpha = 0^\circ$ , and  $Re = 5.1 \cdot 10^6$ : the shaded domain corresponds to the flow field with two local supersonic regions.

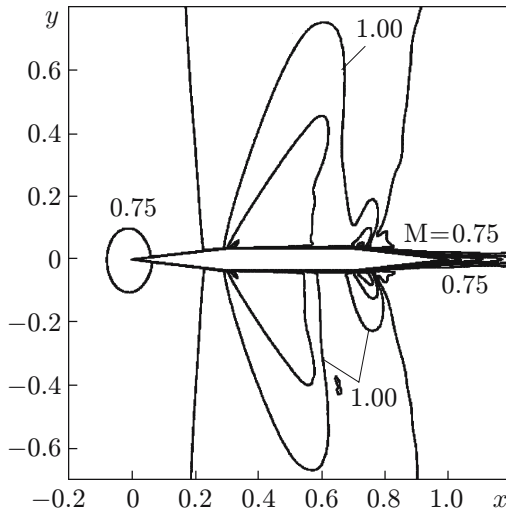


Fig. 6. Mach number contours in an asymmetric flow past the airfoil described by Eqs. (5) with  $h = 0.07$ ,  $a = 0.3$ ,  $\alpha = 0^\circ$ ,  $M_\infty = 0.852$ , and  $Re = 5.1 \cdot 10^6$ .

Figure 5 shows the dependence of the lift coefficient on the Mach number for the airfoil (5) at  $\alpha = 0^\circ$ . Flow bifurcations are revealed in a narrow range of the free-stream Mach numbers

$$0.8511 < M_\infty < 0.8536. \quad (6)$$

To obtain asymmetric flow regimes with a positive lift coefficient, we first ran the solver for the initial data  $M_\infty = 0.853$  and  $\alpha = 0.5^\circ$  and then gradually reduced the angle of attack  $\alpha$  to zero. The resultant asymmetric flow at  $\alpha = 0^\circ$  was used as the initial state for computations of asymmetric flows at smaller and greater values of  $M_\infty$ ; in this way, we determined interval (6). Figure 6 demonstrates the asymmetric flow obtained for  $M_\infty = 0.852$ . The Reynolds number based on the airfoil chord length of 0.5 m and  $M_\infty \approx 0.852$  is  $5.1 \cdot 10^6$ .

A comparison of the numerical results with those presented in [4] for a smooth airfoil shows that the existence of airfoil breakpoints at  $x = 0.7$ ,  $y = \pm 0.035$  entails a shift of the terminating shock waves upstream to the breakpoints and shrinking of the local supersonic regions on both airfoil surfaces. As a result, the correlation of the supersonic regions via the near wake region decreases, and the range of  $M_\infty$ , in which asymmetric regimes exist, becomes narrower.

For  $M_\infty < 0.857$ , there are no self-sustained flow oscillations, as the boundary layer separation from the airfoil is weak in this case. At the same time, reduction of the airfoil nose (tail) length from  $a = 0.3$  to  $a = 0.25$  or a 2.5-fold decrease in pressure  $p_\infty$  (and, hence, in the Reynolds number) would result in excitation of oscillations in both symmetric and asymmetric flow regimes.

**Conclusions.** This study has confirmed the concept proposed in [3–5] that the length of the airfoil midpart with a small or zero curvature is of principal importance for the onset of flow bifurcations. The values of  $M_\infty$  at the beginning of the bifurcation interval turn out to be the most unfavorable ones, because there are considerable jumps of the lift coefficient under small perturbations of the angle of attack at those Mach numbers. The existence of breakpoints at the junction of the airfoil tail and midpart results in shrinking of the bifurcation interval with respect to  $M_\infty$  at  $\alpha = 0^\circ$ .

## REFERENCES

1. M. M. Hafez and W. H. Guo, “Nonuniqueness of transonic flows,” *Acta Mech.*, **138**, Nos. 3/4, 177–184 (1999).
2. M. M. Hafez and W. H. Guo, “Some anomalies of numerical simulation of shock waves. 1. Inviscid flows,” *Comput. Fluids*, **28**, Nos. 4/5, 701–719 (1999).
3. A. G. Kuz’mın, “Bifurcations and buffet of transonic flow past flattened surfaces,” *Comput. Fluids*, **38**, No. 7, 1369–1374 (2009).
4. A. G. Kuz’mın, “Self-sustained oscillations and bifurcations of transonic flow past simple airfoils,” *J. Appl. Mech. Tech. Phys.*, **49**, No. 6, 919–925 (2008).
5. A. G. Kuz’mın, “Bifurcations of transonic flow past flattened airfoils,” Centre pour la comm. sci. directe: <http://hal.archives-ouvertes.fr/hal-00433168/en>.
6. F. Menter, “Zonal two equation  $k-\omega$  turbulence model predictions,” AIAA Paper No. 93-2906 (1993).